Understanding the Link between Strain Transfer and Probability of Detection in Distributed Optical Fiber Sensors

Falcetelli, Francesco; Yue, Nan; Rossi, Leonardo; Bolognini, Gabriele; Bastianini, Filippo; Zarouchas, Dimitrios; Di Sante, Raffaella

DOI
10.1364/OFS.2023.th6.98

Publication date
2023

Document Version
Final published version

Citation (APA)
Falcetelli, F., Yue, N., Rossi, L., Bolognini, G., Bastianini, F., Zarouchas, D., & Di Sante, R. (2023). *Understanding the Link between Strain Transfer and Probability of Detection in Distributed Optical Fiber Sensors*. Paper presented at 28th International Conference on Optical Fiber Sensors, OFS 2023, Naka-ku, Hamamatsu-shi, Japan. https://doi.org/10.1364/OFS.2023.th6.98

Understanding the Link between Strain Transfer and Probability of Detection in Distributed Optical Fiber Sensors

Francesco Falcetelli [1,2], Nan Yue [3], Leonardo Rossi [2], Gabriele Bolognini [2,*], Filippo Bastianini [4], Dimitrios Zarouchas [5] and Raffaella Di Sante [1]

[1]Department of Industrial Engineering—DIN, University of Bologna, 47121 Forlì, Italy;
[2]IMM Institute, Consiglio Nazionale delle Ricerche, 40129 Bologna, Italy;
[3]Department of Aerospace Structures and Materials, Faculty of Aerospace Engineering, Delft University of Technology, 2629 HS Delft, The Netherlands;
[4]SOCOTEC Photonics, 40069 Zola Predosa, Italy;
[5]Center of Excellence in Artificial Intelligence for Structures, Prognostics & Health Management, Aerospace Engineering Faculty, Delft University of Technology, Kluyverweg 1, 2629 HS Delft, The Netherlands;
[*]bolognini@bo.imm.cnr.it

Abstract: The research shows the link between the strain transfer properties of distributed optical fiber sensors and their probability of damage detection, which is crucial for a successful implementation in real structural health monitoring applications. © 2023 The Authors

1. Introduction

Distributed Optical Fiber Sensors (DOFSs) allow to simultaneously acquire strain distributions over the entire length of a sensing optical fiber with varying degrees of spatial resolution, range, and accuracy depending on the interrogation system and the scattering phenomenon they are based on (Rayleigh, Brillouin, or Raman) [1,2]. These features make DOFSs prime candidates for employment in many Structural Health Monitoring (SHM) applications. Still, their successful implementation in this field depends on a clear characterization of their damage detection capabilities. Such characterization can be achieved by developing methodologies to extract Probability of Detection (POD) curves which translate the system sensing performance into its reliability in detecting specific types of damage. Even though such methodologies are already well-established, such as the ones found in MIL-HKBK-1823A [3], they are designed for a different sensing approach, namely Non-Destructive Evaluation (NDE). These protocols are incompatible with SHM, since it relies on permanently installed sensors, includes additional sources of variability compared to NDE, and produces a series of spatial and time correlated data [4,5]. Despite this, it is possible to produce POD curves for DOFSs by relying on statistical models specifically designed for SHM such as The Length at Detection (LaD) and Random Effects Model (REM) [6].

In real SHM applications, the damage detection capability of a DOFSs-based system also depends on factors such as measurement noise, loading conditions, geometrical properties of the structure, morphology of damage, environmental and operational conditions (EOCs), and human factors. In addition, it can also depend on the sensing fiber in terms of strain transfer efficiency, which defines how the strain from the structure is transferred to the sensing fiber core, where the strain is effectively measured. This value depends on the geometrical and mechanical properties of the sensing fiber [7], and degrades with the addition of protective layers between the fiber and the structure. Despite this, protective layers are necessary to ensure long-term durability of the fiber.

In this work, we evaluate how the combined effects of different strain transfer efficiencies and measurement noise influence the POD curves developed for DOFSs. The study makes use of a Model-Assisted POD (MAPOD) framework developed in Falcetelli et al. [8], recreating different POD curves for varying values of noise and strain transfer.

For DOFS systems capable of performing dynamic strain measurements, the estimation of how the POD evolves with varying strain transfer properties of the sensing fiber and noise can be particularly useful. For example, in the case of sensors based on Swept Wavelength Interferometry (SWI) [9], like the ODiSI-B developed by LUNA Innovations Inc. [10], frequencies of up to 250 Hz can be reached. If the noise levels are found to degrade the POD, they can be reduced by averaging multiple measurements, thus creating the opportunity of trading improved POD for reduced sampling rate of the sensor, thus increasing the range of applicability of these technologies.

2. Materials and Methods

The strain transfer effect can be modeled by means of the system transfer function, Γ, which can be thought of as the DOFS response after a Dirac strain impulse.

$$\Gamma(x) = \frac{1}{2\lambda} e^{-\frac{x}{\lambda}}, \tag{1}$$

where λ represents the space constant parameter [8]. This parameter is the inverse of the shear lag parameter, which was described in several strain transfer studies [7,11,12]. Then, in the most general case, the strain profile in the optical fiber core, $\varepsilon_f(x)$, can be computed as a convolution operation between the strain profile in the structure, $\varepsilon_s(x)$, and the system transfer function, Γ:

$$\varepsilon_f(x) = (\Gamma \otimes \varepsilon_s)(x). \quad (2)$$

Fig.1 shows the DOFS response (blue line) to a rectangular strain profile input (dashed black line), and the system transfer function (red dashed line).

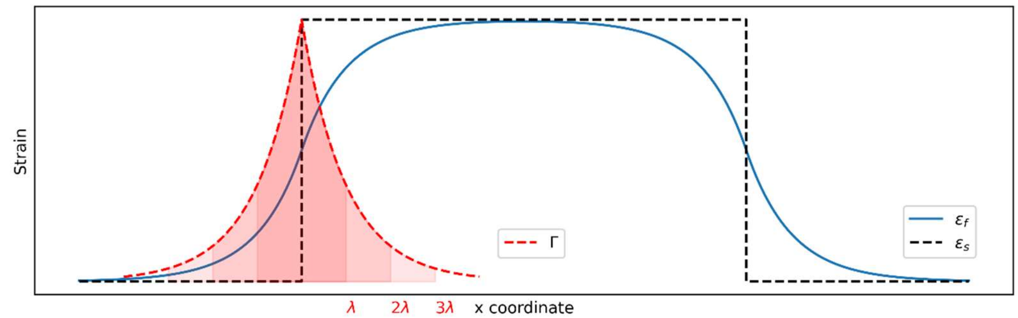

Fig. 1. Strain transfer effect on the measured strain profile. At 3λ approximately 97% of the strain has been transferred from the structure to the DOFS core.

To simulate the POD at different levels of transfer efficiency and measurement noise, the authors employ the MAPOD developed in [8]. This MAPOD approach allows to simulate the response of a DOFS which is monitoring the crack growth from an initial length a_0 to a final length a_f, in a carbon fiber reinforced polymer (CFRP) double cantilever beam (DCB) specimen undergoing quasi-static loading (see Fig. 2). The model was validated with an equivalent experimental setup using the ODiSI-B as interrogator [13]. These kinds of structure and damage are representative of many composite components used in aircraft structures subjected to delamination.

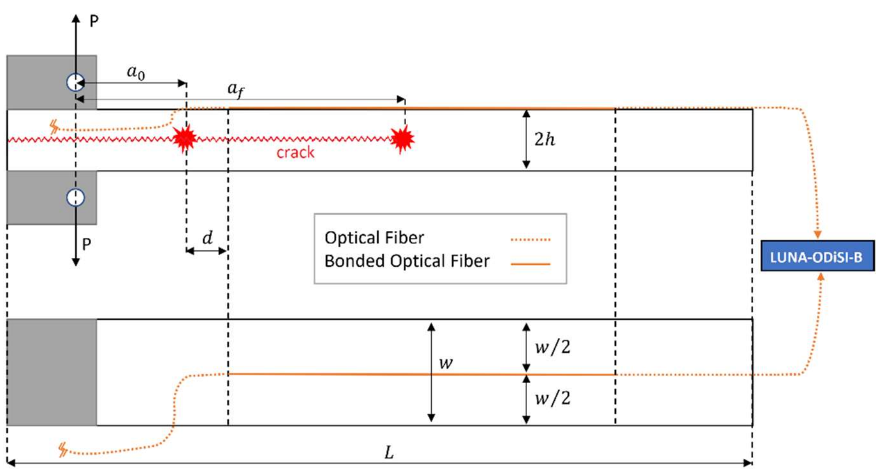

Fig. 2. DCB and DOFS bonding scheme in the MAPOD framework.

The model can produce a MAPOD curve for a given parameter configuration. Fig. 3 shows an example of a MAPOD curve obtained using the LaD method and its lower bound obtained with the one-sided tolerance interval (OSTI) approach [14]. The quantities of interest for the reliability assessment are a_{90} and $a_{90/95}$. The former represents the damage size that can be detected with a probability of 90%, whereas the latter denotes the damage size that can be detected with a probability of 90% with a confidence of 95%.

3. Results

In this study, POD curves were computed for different λ values in the model. Specifically, λ was swept from 0.01 mm to 100 mm with 100 intervals evenly distributed on a geometric scale. Fig. 4 shows the results of these simulations, plotting a_{90} and $a_{90/95}$ against λ for a scenario where the noise equals 30 με. Both a_{90} and $a_{90/95}$ can be fitted with an exponential law. However, since $a_{90/95}$ is taken as the reference reliability metric, Fig. 4 shows only the exponential fitting related to $a_{90/95}$, drawn with a blue-dashed line.

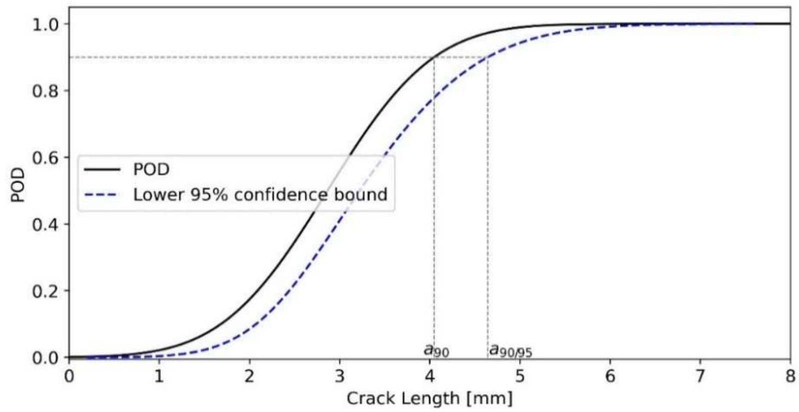

Fig. 3. Example of MAPOD curve and its lower bound.

It is possible to extrapolate two relevant quantities for the space constant: λ_1 and λ_2. The space constant equals λ_1 when the $a_{90/95}$ fit line increases of 20% from its initial value. Although the choice of considering a 20% increase is arbitrary, λ_1 can be seen as a critical value above which the detection performance of the system rapidly degrades. On the other hand, the space constant equals λ_2 when the $a_{90/95}$ fit line reaches 10 mm. This value of 10 mm is also chosen arbitrarily, but in general can be thought of as the critical $a_{90/95}$ for a specific SHM application. Thus, λ_2 is the ultimate admissible space constant value for a given application.

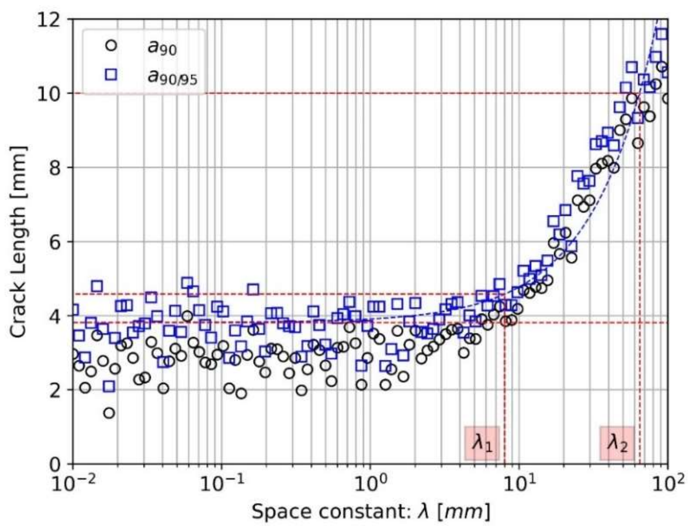

Fig. 4. Sensitivity of a_{90} and $a_{90/95}$ to the strain transfer space constant λ with a noise value of 30 $\mu\varepsilon$. The lowest red-dashed line represents the initial value for the $a_{90/95}$ fit line. The second red-dashed line represents an increase of 20% from the lower line. The highest red-dashed line is drawn at a critical crack length of 10 mm.

Fig. 5 plots the λ_1 and λ_2 obtained repeating the abovementioned procedure for several noise values. As is expected, the higher the noise level, the lower the λ_1 and λ_2 which are allowed, resulting in stricter requirements for the sensing fibers in terms of strain transfer quality. In more detail, the relations between λ_1 and λ_2 seem to both follow a power law. For a given DOFS, thus for a given space constant λ, the information in Fig. 5 can be used to find the noise tolerance for λ_1 and λ_2. If the noise tolerance is greater or equal to the measured noise level, the optical fiber meets the requirements. On the contrary, if the resulting noise level is lower than the measured noise level, there are two possible solutions. The first is simply to substitute the optical fiber with another having a lower strain transfer space constant hence better stain transfer performance. The second is to perform repeated measurements, leveraging the central limit theorem to reduce the noise. If the results are averaged over n measurements, the resulting noise will be $\sigma_X = \sigma/\sqrt{n}$. As a tradeoff, the sampling rate is reduced by the factor $n = (\sigma/\sigma_X)^2$.

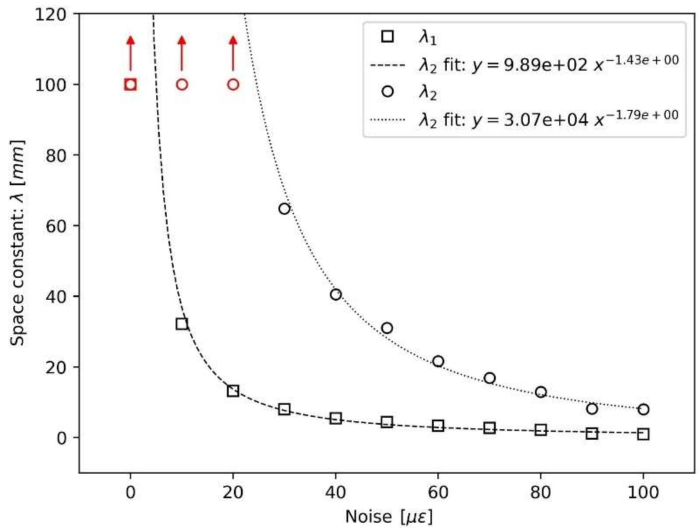

Fig. 5. Trends of λ_1 and λ_2 as a function of noise. The red markers represent space constant values greater than 100 mm and thus outside the λ sweep range.

4. Conclusions

This study exemplifies a way of quantifying the influence of the strain transfer of DOFSs on their relative POD, providing information on the reliability of the system in terms of damage detection for a given SHM application at different noise levels. As said in the introduction, this evaluation can also provide practical guidelines and to find the optimal tradeoff between measuring accuracy and sampling frequency for a certain DOFS given the critical space constant values λ_1 and λ_2. These guidelines have the potential to extend the range of application of DOFS technologies, by providing insight which can be used to enable reliable measurements where either high noise levels or poor strain transfer properties would otherwise prevent to do so. Further studies should be devoted to similar considerations applied to other critical parameters such as loading conditions and geometrical properties of the structure, damage morphology, EOCs, and human factors.

5. Acknowledgements

This activity has received funding from the European Union through Horizon 2020, the Framework Programme for Research and Innovation, under project SLAM DAST, Grant Agreement No. 971149.

6. References

[1] P. Lu, N. Lalam, M. Badar, B. Liu, B. T. Chorpening, M. P. Buric, and P. R. Ohodnicki, "Distributed optical fiber sensing: Review and perspective," Applied Physics Reviews **6**, 041302 (2019).

[2] F. Bastianini, R. Di Sante, F. Falcetelli, D. Marini, and G. Bolognini, "Optical fiber sensing cables for Brillouin-based distributed measurements," Sensors **19**, 5172 (2019).

[3] *Department of Defense Handbook: Nondestructive Evaluation System Reliability Assessment* (Department of Defense, 2009).

[4] C. M. Schubert Kabban, B. M. Greenwell, M. P. DeSimio, and M. M. Derriso, "The probability of detection for structural health monitoring systems: Repeated measures data," Structural Health Monitoring **14**, 252–264 (2015).

[5] F. Falcetelli, N. Yue, R. Di Sante, and D. Zarouchas, "Probability of detection, localization, and sizing: The evolution of reliability metrics in Structural Health Monitoring," Structural Health Monitoring (2021).

[6] W. Q. Meeker, D. Roach, and S. S. Kessler, "Statistical Methods for Probability of Detection in Structural Health Monitoring," in *Structural Health Monitoring 2019* (DEStech Publications, Inc., 2019).

[7] F. Falcetelli, L. Rossi, R. Di Sante, and G. Bolognini, "Strain Transfer in Surface-Bonded Optical Fiber Sensors," Sensors **20**, 3100 (2020).

[8] F. Falcetelli, N. Yue, L. Rossi, G. Bolognini, F. Bastianini, D. Zarouchas, and R. D. Di Sante, "A Model-Assisted Probability of Detection Framework for Optical Fiber Sensors," Sensors **23**, 4813 (2023).

[9] E. D. Moore and R. R. McLeod, "Correction of sampling errors due to laser tuning rate fluctuations in swept-wavelength interferometry," Opt. Express **16**, 13139 (2008).

[10] *Optical Distributed Sensor Interrogator Model ODiSI-B: User's Guide* (Luna Innovations Inc., 2017).

[11] H. Wang and Z. Zhou, "Advances of strain transfer analysis of optical fibre sensors," Pacific Science Review **16**, 8–18 (2014).

[12] A. Billon, J.-M. Hénault, M. Quiertant, F. Taillade, A. Khadour, R.-P. Martin, and K. Benzarti, "Qualification of a distributed optical fiber sensor bonded to the surface of a concrete structure: a methodology to obtain quantitative strain measurements," Smart Mater. Struct. **24**, 115001 (2015).

[13] F. Falcetelli, D. Cristiani, N. Yue, C. Sbarufatti, E. Troiani, R. Di Sante, and D. Zarouchas, "Qualification of distributed optical fiber sensors using probability of detection curves for delamination in composite laminates," Structural Health Monitoring 147592172211411 (2022).

[14] D. Roach, "Real time crack detection using mountable comparative vacuum monitoring sensors," Smart Structures and Systems **5**, 317–328 (2009).